Investigation on the Effect of Cable Length on Pulse Shape of High Voltage High Pulse Power Supply

Krishna Kumar Rai,[#,*] A.V. Giridhar,[$] D.R. Jahagirdhar,[%] Ashish Rai,[^] and Akash Kumar Paul[$]

[#]DRDO-Center For High Energy Systems and Sciences, Hyderabad - 500 053, India
[$]Electrical Department, NIT, Warangal - 506 004, India
[%]DRDO-Research Center Imarat (RCI), Hyderabad - 500 069, India
[^]DRDO-SF Complex, Jagdalpur, India
[*]E-mail: kkrai@chess.drdo.in

ABSTRACT

In the present scenario of pulse power applications, transmission of high voltage pulses varies as per load condition. In the early days of its application, High Voltage High Pulse Power Supply (HVHPPS) design saw short distance between load and source, where the effect of cable length was not taken into account for design. This paper presents the effect of cable length on pulse shape of High Voltage High Pulse Power Supply. The load under observation is Klystron based high energy particle accelerator system. The performance of pulse power systems were observed continuously on a daily basis throughout the year and detailed analysis was carried out. This paper generates the model of pulse forming system and provides details of pattern distortion of the pulse shape due to various dynamic parameter changes i.e. impedance, Load Voltage, Load Current, Cavity Dimensional Changes (Microwave components) due to temperature variations and performance of the power supply. The results were analysed and validated with hardware results across a range of actual industrial loads.

Keywords: Pulse shape; High voltage high pulse power supply; Impedance matching

1. INTRODUCTION

High Voltage High Pulse Power Supply has commercial, medical, research and industrial applications. In industrial applications, where high voltage high pulse power needs to be transmitted across long distances, the length of transmission line has significant effect on the shape of high voltage pulses. High Voltage High Pulse Power Supply compresses energy into peak power of a single pulse at a selectable PRF (Pulse Repetition Frequency). This HVHPPS is used for pulsed applications i.e. in magnetron, klystron, accelerators etc. The performance would be better if pulse to pulse regulation and impedance matching is achieved. The use of HVPPS is divided into two categories, the first category involves nuclear system and linear accelerators. The second category is pulse power modulators and line pulser, derived from pulsed radar[1,9].

Any power system in a miniaturised form is always welcome for defence, space and commercial applications. The five building blocks in any pulse power system are; Power Source (i.e Battery, MHD, Fuel Cell Generation), Pulse compress and Pulse formation circuit, Impedance matching, pulse boosting and types of loads as illustrated in Fig. 1.[5,8]

2. PFN AND TRANSMISSION LINE

Characteristic impedance of transmission line is measured at the end of infinite length. The characteristic impedance is equal to PFN impedance which is derived from load impedance as per design. In equilibrium condition all the energy flowing through the line is absorbed at the termination and none is dissipated[6].

Line type pulser is a Pulse Forming Network, used for the formation of pulse. The PFN stores the energy which generates a pulse and discharges this energy into a load of specified shape and time duration of pulse. This energy is effectively stored in a capacitor bank as shown in Figure 2.

In initial state the current begins to charge each capacitor through the series inductor of each section of the network. The result is that each capacitor will charge to the voltage 2Edc at a charging time that is increasingly longer for each capacitor down the network[7].
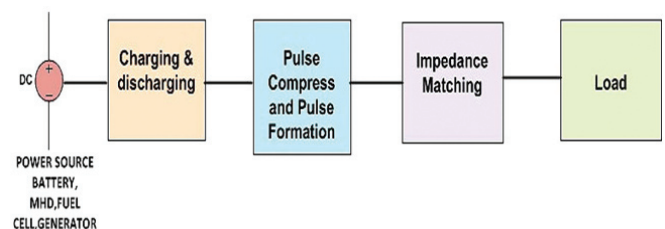
Figure 1. Building blocks of HVHPPS.
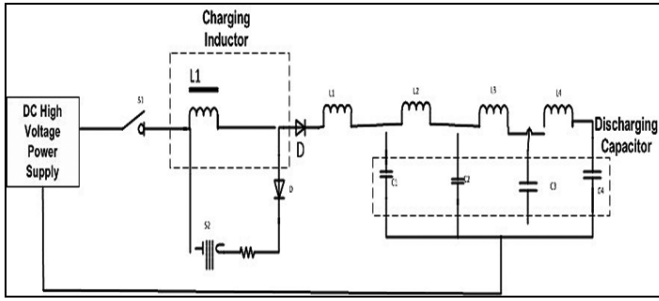
Figure 2. Resonant charging with PFN.

3. FORMATION AND SHAPING OF PULSES

There are various topologies for pulse power generation such as superconductor based repetitive inductive pulse power supply and Pulse Forming Network (PFN) for arbitrary pulse generation. Most pulser systems are designed to achieve rectangular pulse through lossless transmission line i.e PFN. The transient produced by the discharge circuit of line into a resistance load is as shown in Fig. 3.
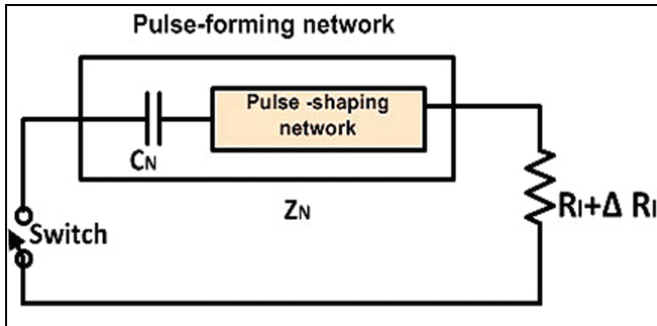
Figure 3. Schematic diagram for producing rectangular pulse from a transmission line.

Impedance based on the transmission line theory is as follows,

$$Z = Z_\circ \coth j\omega\delta \qquad (1)$$

The Laplace-transform impedance after substituting $j\omega$ with p (transform parameter)

$$Z(p) = Z_\circ \coth p\delta \qquad (2)$$

Where, δ is one-way transmission time and $Z_\circ$ is characteristic impedance. $i(p) = \dfrac{V_\circ}{p(R_\ell + Z_\circ \coth p\delta)}$

$$= \frac{V_\circ}{p(Z_\circ + R_\ell)} \bullet \frac{1 - e^{-2p\delta}}{1 + \dfrac{Z_\circ - R_\ell}{Z_\circ + R_\ell} e^{-2p\delta}} e^{-2p\delta}$$

$$= \frac{V_\circ(1 - e^{-2pV})}{p(Z_\circ + R_\ell)} \left[\begin{array}{l} 1 - \dfrac{Z_\circ - R_\ell}{Z_\circ + R_\ell} e^{-2p\delta} \\ + \left(\dfrac{Z_\circ - R_\ell}{Z_\circ + R_\ell} \right)^2 e^{-4p\delta} - .... \end{array} \right] \qquad (3)$$

Where, $V_\circ$ initial voltage of network. The inverse transform gives the current as,

$$i(t) = \frac{V_\circ}{Z_\circ + R_\ell} \left\{ \begin{array}{l} 1 - U(t - 2\delta) - \dfrac{Z_\circ - R_\ell}{Z_\circ + R_\ell} \\ [U(t - 2\delta) - U(t - 4\delta)] + \\ \left(\dfrac{Z_\circ - R_\ell}{Z_\circ + R_\ell} \right)^2 [U(t - 4\delta) - U(t - 6\delta)] - \end{array} \right\} \qquad (4)$$

Where, $U(\Delta t) = 1$ for $\Delta t > 0$

$U(\Delta t) = 0$ for $\Delta t < 0$

$\Delta t = (t - n\delta)$, $n = 2, 4, 6...$

If $R_\ell = Z_\circ$, if load is matched to the line, the current of a single pulse $I_\ell = \dfrac{V_\circ}{2Z_\circ}$ at $t = 2\delta$. Current and voltage pulse for $R_\ell = Z_\circ$, $R_\ell = 2Z_\circ$ and $R_\ell = \dfrac{1}{2}Z_\circ$ are shown in Fig. 4.
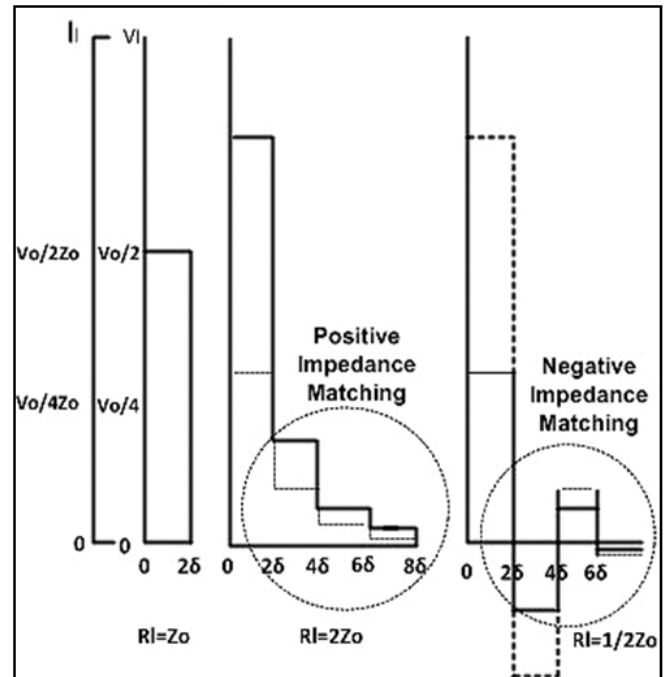
Figure 4. Current and voltage pulses for a lossless transmission line.

Series of steps into of transient discharge at the output pulse is due to mismatch of the load. All steps sign remains same when $R_\ell > Z_\circ$ and opposite sign when $R_\ell < Z_\circ$ as shown in Figure 4. The steps are due to reflections at end of the transmission line by mismatched load Impedance. If transverse time to the load end is δ and reflected travel time to the load end and back will be 2δ, where positive or negative steps are the effect of mismatch ratio. The reflections continue till energy stored in the line is dissipated to the load. Both the design and operation of PFN are affected by reflections.

One-way transmission time of δ gives pulse width of 2δ; assume pulse width of 6μsec duration and a signal speed

on the line of 500m/ μsec (assumed value), a line of length

$l = 500 X \dfrac{6}{2} = 1500m$ is required. Thus, such line length will

be unrealistic for pulse forming network due to large size and weight, where impedance are matched throughout the line. Pulse deformation will take place if and only if the impedance are not matched. During transmission of pulse for varying length will have impact on pulse shape at the trailing end only.

4. NETWORKS DERIVED FROM A TRANSMISSION LINE

For implementation of PFN circuit, distributed parameters give partial differential equations, whereas lumped-parameters give differential equations. The true pulse definition will improve as the number of distributed parameters i.e. number of elements increased[2-3,10].

The transmission line equivalent of two-terminal line-simulating network as shown in Fig. 5.
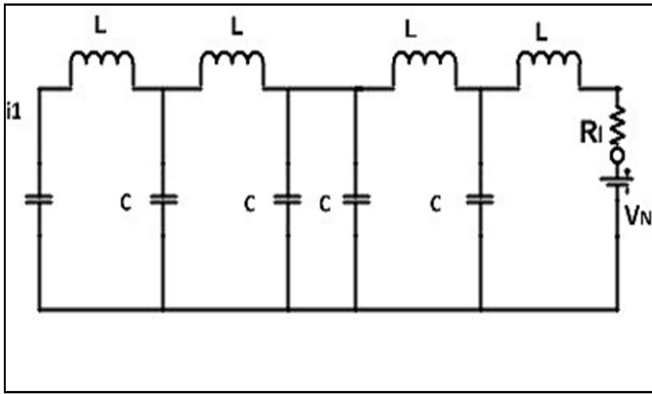
Figure 5. Two terminal line-simulating network.

We assume the following:

$$\dfrac{i_{r-1}(p)}{C_p} + \left(L_p + \dfrac{2}{C_p}\right) i_r(p) - \dfrac{i_{r+1}(p)}{C_p} = 0 \qquad (5)$$

Where, r is the rth mesh. The differential equation is:

$$i_r(p) = Ae^{r\theta} + Be^{-r\theta} \qquad (6)$$

Where $\cosh \theta = 1 + \left(\dfrac{LC}{2}\right) p^2$,

A and B = arbitrary constants, this can be find out by mesh equations. Consider first the case for which resistance R_ℓ, in series with the battery V_N, is zero. The current flows after closing the switch indefinitely and represents a steady-state instead of a transient condition. Transient current occurs if dissipative elements are there. The hyperbolic function for equation 6 will be as shown below:

$$i_1(p) = CV_N \dfrac{\sinh n\theta}{\sinh(n+1)\theta - \sinh n\theta}$$

Input – impedance transform for the network as shown in Eqn. 7.

$$Z(p,n) = \dfrac{V_N}{p i_1(p)} = \dfrac{1}{C_P} \left[\dfrac{\sinh(n+1)\theta}{\sinh(n\theta)} \right] \qquad (7)$$

The limit of $Z(p,n)$ as n approaches infinity since number of inductance and capacitance are fixed so that total inductance and capacitance of network is also be fixed[4].

$$\lim_{n\to\infty} z(p,n) = \lim_{n\to\infty} \dfrac{1}{Cp} \left[\dfrac{\sinh(n+1)\theta}{\sinh(n\theta)} - 1 \right]$$

$$= \lim_{n\to\infty} \dfrac{1}{Cp} \left[\cosh \theta + \coth n\theta \sinh \theta - 1 \right]$$

But,

$$\cosh \theta = 1 + \dfrac{LC}{2} p^2 = 1 + \dfrac{L_N C_N}{2n^2} p^2,$$

$$\sinh \theta = \sqrt{\cos h^2 \theta - 1}$$

$$= \dfrac{\sqrt{L_N C_N}}{n} p \sqrt{1 + \dfrac{\sqrt{L_N C_N}}{4n^2} p^2}$$

$$n\theta = 2n \sin h^{-1} \dfrac{\sqrt{L_N C_N}}{2n} p$$

This gives,

$$\lim_{n\to\infty} = Z(p,n) = \lim_{n\to\infty} \dfrac{n}{C_{Np}} \left[\dfrac{\dfrac{L_N C_N}{2n^2} p^2 + \dfrac{\sqrt{L_N C_N}}{n} p}{\sqrt{1 + \dfrac{L_N C_N p^2}{4n^2}} \coth \left[(2n \sin h^{-1} \sqrt{L_N C_N} p) \right]} \right]$$

$$= \sqrt{\dfrac{L_N}{C_N}} \bullet \coth p \sqrt{L_N C_N}$$

$$= Z_N \coth p\delta \qquad (8)$$

Equation 8 represents impedance function of transmission line. The pulse shape generated by the simulating line network

on matched resistance load, $R_\ell = \sqrt{L_N C_N} = \sqrt{\dfrac{L}{C}}$, may be found by charging-current when V_N is applied to the circuit. If the voltage transform is divided by the addition of the load resistance and the network impedance then we obtain:

$$i_1(p) = \dfrac{\dfrac{V_N}{p}}{\sqrt{\dfrac{L}{C}} + \dfrac{1}{C_P} \bullet \dfrac{\sinh(n+1)\theta}{\sinh(n\theta)} - 1}$$

But from the value of θ

$$P = \frac{2}{\sqrt{LC}} \sin h_2 \theta$$

Hence,

$$i_1(p) = CV_N \frac{\sinh n\theta}{\sinh(n+1)\theta + (2\sinh\frac{\theta}{2} - 1)\sinh n\theta} \quad (9)$$

Eq. (9) is true for number of sections n. The simplest form occurs when $n = 1$. Here,

$$i_1(p) = CV_N \frac{\sinh \theta}{\sinh 2\theta + (2\sinh\frac{\theta}{2} - 1)\sinh \theta}$$

$$= \frac{V_N}{L} \bullet \frac{1}{p^2 + \frac{1}{\sqrt{LC}}p + \frac{1}{LC}} \text{ is the current transform}$$

for a one mesh RLC-circuit where $R = \sqrt{\frac{L}{C}}$ ..

This method is derived in Eq. (10), the limit of $i_1(p)$, as n reaches to infinity then total distributed capacitance C_N and the total distributed inductance L_N will be fixed for large number of distributed parameters as shown below:

$$\lim_{n\to\infty} i_1 p = \frac{V_N}{\sqrt{\frac{L_N}{C_N}}p} (1 - e^{-2\sqrt{L_N C_N}p}) \quad (10)$$

The Laplace transform of rectangular current pulse is,

$$\frac{V_N}{2\sqrt{\frac{L_N}{C_N}}p} \text{ and of duration } 2\sqrt{L_N C_N} \;.$$

Both calculated and experimental pulse shape can be predicted for n=6 uniform distributed network on matched impedance load i.e. $R_l = Z_N$. The calculated pulse shape can be found by using Eq. (9) with n=6. It is required to convert from the hyperbolic to the algebraic form corresponding to Eq. (9) then the denominator is 12th degree (=2n). The corresponding experimental pulse shapes, shown, was acquired by an experimental network, thus the actual values of all the parameters were within few percent of the theoretical values. The only difference present in the initial overshoot for which the calculated value is approximately more than the experimental value. This difference occurs because of the gas filled– thyratron switch used line type pulse circuit which does not close instantly.

5. EXPERIMENTAL RESULTS AND ANALYSIS

An experimental hardware developed for varying the length of the tri-axial cable between pulse forming network and klystron load. Also a High Voltage High Pulse Power Supply is developed and tested with a 1.5kΩ resistor connected over four tri-axial cables each having 50Ω line impedance. The overall equivalent impedance of transmission line will be 12.5Ω. Figure 6 shows functional block of experimental hardware.
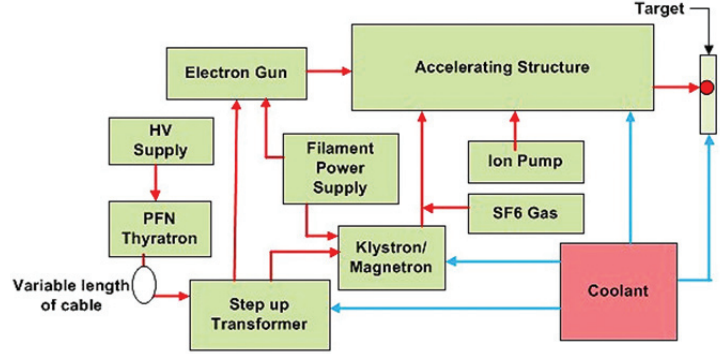
Figure 6. Block diagram of experimental hardware.

Table 1. Hardware specification

Parameter	Value
Pulse Output Voltage	12 kV
Output Current	1000 A
Pulse width (Variable)	6 μsec
Repetition rate (Variable)	10-200Hz
Load impedance(R_L)	12.5 Ω
Turns Ratio of Pulse Transformer	1:10
Duty Cycle	0.001

The overall hardware specification system mentioned in Fig. 1 is shown in Table 1.

The inside view of high voltage high pulse power supply is shown in Fig. 7. The system is energized by three phase 415VAC each time for a particular cable length; vital waveforms i.e. charging voltage, discharging voltage are captured by Yokogawa DL1520 and Tektronix TD1002. In this way the cable length is varied for ten different values and its
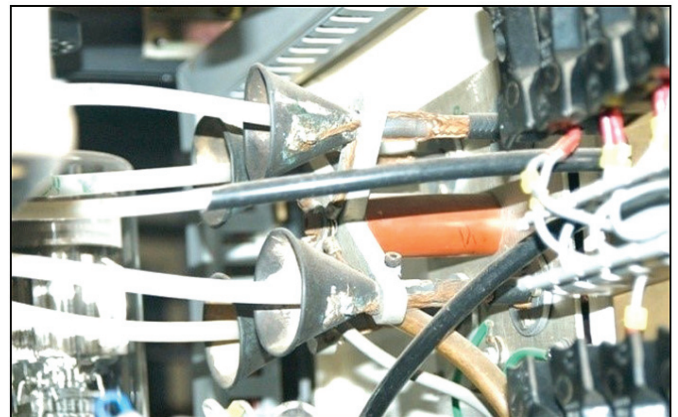
Figure 7. Photograph of cone structure of discharge of high voltage high pulse power supply (HVHPPS).

effect on High Voltage High Pulse Power Supply is captured.

The degree of simulation will improve as the number of elements increases for the given network type. The PFN output pulse will be approximately equal to rectangular pulse network pulse is a good approximation of the rectangular pulse only during the pulse interval. The network pulse may show undershoot, overshoot and varying oscillations, at the beginning and end of the pulse. The pulse shapes were obtained for six uniform section pulse forming network supplied to matched resistance load, when $R_\ell = Z_N$. The calculated and experimental pulse shapes are very close and the major difference is in the initial overshoot, so the calculated value is approximately twice the observed value. The experiment is done on 12KV of HVDC @ 7.0 Amps of charging current, to get a pulse of 12.0 KV rectangular shapes for 6 micro seconds for the above mentioned Pulse Forming Network configuration. The actual hardware of 12KV pulse output PFN based modulator as shown in Fig. 8 is used for the experiment.

Figure 8. Experimental modulator hardware.

In this experiment, all the time cable length of the system changes and cable connection for high voltage supply is ensured. In this case, klystron of 6MWatt peak power and 6kW average power has been taken into account and the results were obtained experimentally.
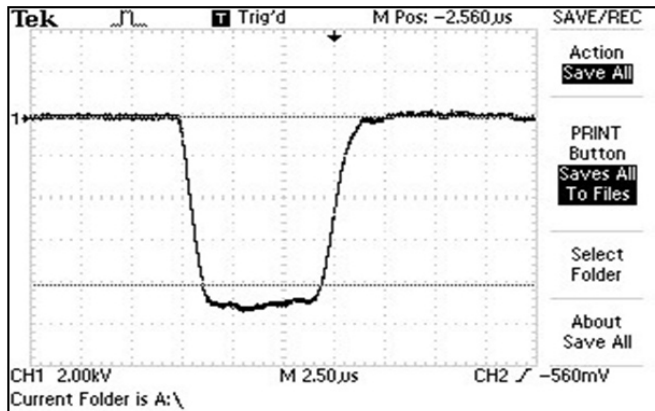
Figure 9. Length of cable: high voltage pulse with 10 meters.

When the length is less, the top of the pulse is found to be flat in shape. The initial overshoot and undershoot is at a minimum level and as per calculated value. As the length of the tri-axial cable is less, the load impedance is lower and, the mismatch is also minimum.
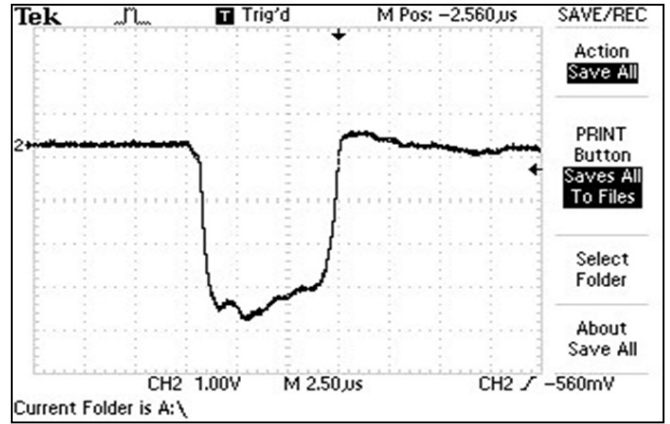
Figure 10. Length of cable: high voltage pulse with 30 meters.

When the length is increased moderately, the top of the pulse is disturbed by ripples. The initial overshoot and undershoot increase moderately. The load impedance changes

as per $\sqrt{\dfrac{L_N}{C_N}}$ with an experimental change of $\sqrt{\dfrac{L_N + \Delta L}{C_N + \Delta C}}$ and accordingly, the pulse width ($2\sqrt{L_N C_N}$) change is negligible, whereas the amplitude of the pulse shows marginal reduction due to waveform distortion compared to earlier flat top wave shape.

As per the derivation, the pulse current $\dfrac{V_N}{2\sqrt{\dfrac{L_N}{C_N}}}$ changes due to the impact of impedance change.
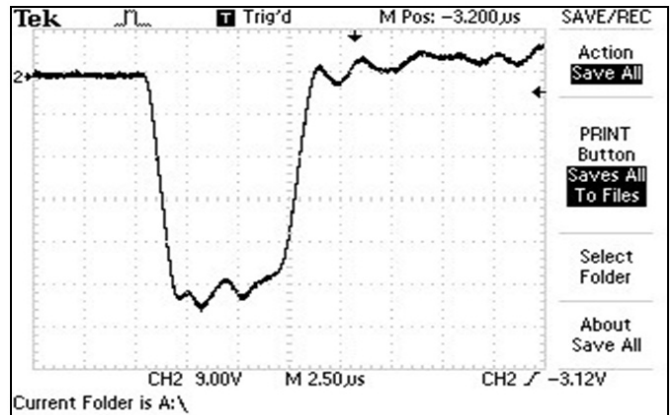
Figure 11. Length of cable: High voltage pulse with 50 meters.

When the length is increased further, the top of the pulse is disturbed by ripples and negative mismatch. If we compare the Pulse shape parameter with earlier wave forms at 30 m cable length, as the length we find that increased, pulse width also increased i/e the pulse current amplitude had significant reduction.

The phenomena still follows the same pattern like the rectangular portion of the wave and the quantity of the overshoot and undershoot (Fig. 12). After microscopic analysis
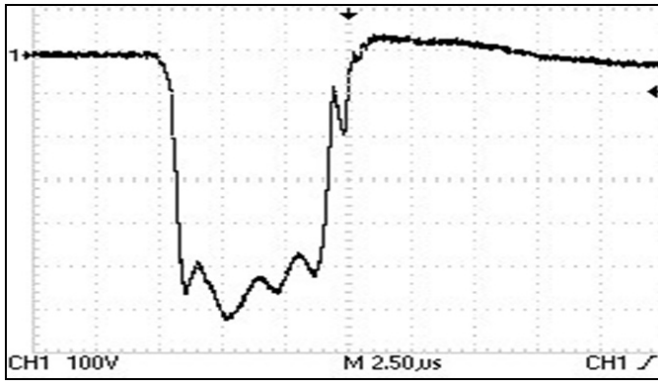
Figure 12. Length of cable: high voltage pulse with 70 meters.

of wave shape, it is found that average pulse current amplitude has significant reduction compared to 50m of cable length pulse current, while pulse width reports marginal changes.

Figure 13 shows pulse shape was distorted badly at the same time that the pulse flat top was disturbed. The pulse width also got changed and average pulse current had drastic reduction due to incorporation of ΔL and ΔC. This type of pulse shape utilization will not be effective for microwave power generation.
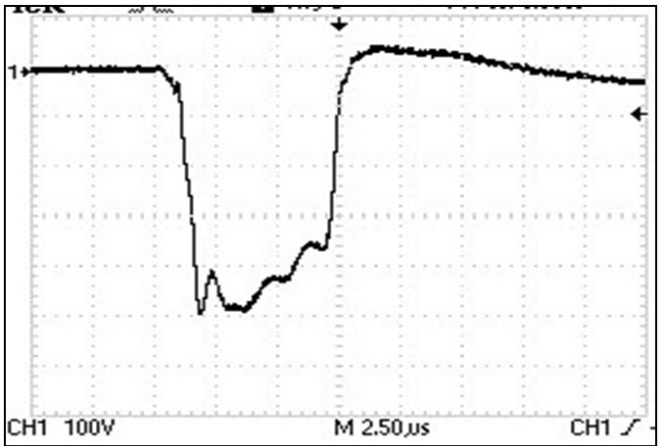
Figure 13. Length of cable: high voltage pulse with 90 meters.

Table 2. Comparative analysis of wave shape and mismatch

Length of cable (m)	Initial over shoot (%)	Under shoot (%)	Type of mismatch
10	Minimum	Minimum	Matched
30	< 01	< 0.5	Negative
50	< 03-04	< 01-02	Negative
70	< 06-07	< 03-04	Negative
90	< 10	< 6	Negative

6. CONCLUSION

It is observed that the shape of the discharge pulses is varying systematically with respect to length of cable. Initial pulse flat top spikes are due to impedance mismatch and not due to triggering effect of switches. Hence, pulse shaping

could be improved by proper impedance matching between the pulse forming network and load. From the above experimental study, it is concluded that as the length of cable increases the impedance matching deteriorates and the pulse generation is affected. There is ample scope to study active pulse shaping of Pulse forming network for variable load and variable length application.

The cable length should be so varied that flexibility is ensured at the time of hardware design so as to ensure variable pulse power transmission; optimization of length of cable is also possible to utilize pulse power transmission in a profitable manner.

REFERENCES

1. Haitao, Li; Zhongming, Yan; Cunshan, Zhang; Yu, Wang; Mingliang, Gao & Guofeng, Zou. Experimental study of inductive pulsed power supply based on multiple HTSPPT Modules. *IEEE TPS*, 2016, **44**(6), 950-956. doi: 10.1109/TPS.2016.2558663.
2. Falong, Lu; Xinyi, Nie; Yu, Wang; Weirong, Chen & Zhongming, Yan. Influence of the mutual inductance between two HTSPPT modules on three discharge modes of superconducting pulsed power supply. *IEEE TPS*, 2018, **46**(8), 2993-2998. doi:10.1109/TPS.2018.2852706.
3. Zhenmei, Li; Haitao, Li; Xiaotong, Zhang; Cunshan, Zhang; Shucun, Liu & Tong, Lu. Modeling and simulation of railgun system driven by multiple HTSPPT modules. *IEEE TPS*, 2018, **46**(1), 167-174. doi:10.1109/TPS.2017.2777699.
4. Sizhuang, Liang; Youtong, Fang & Xiaoyan, Huang. Simulation of an electromagnetic launcher with a superconducting inductive pulsed power supply. *IEEE TAS*, 2016, **26**(4). 1-1. doi:10.1109/TASC.2016.2521427.
5. Falong, Lu; Yu, Wang; Xiufang, Wang; Xiaoyong, Liao; Zhengyou, He & Zhongming, Yan. Study on the collaborative discharge of a double superconducting pulsed power supply based on HTSPPT Modules. *IEEE TAS*, 2017, **99**(1-1). doi:10.1109/TASC.2017.2776269.
6. Haitao, Li; Yadong, Zhang; Cunshan, Zhang; Mingliang, Gao; Yunzhu, An & Tao, Zhang. A repetitive inductive pulsed power supply circuit topology based on HTSPPT. *IEEE TPS*, 2018, **46**(1), 134-139. doi:10.1109/TPS.2017.2776564
7. Haitao, Li; Cunshan, Zhang; Zhenmei, Li; Yuanchao, Hu; Mingliang, Gao & Xinxin, Zheng. An inductive pulsed-power supply circuit consisting of multiple HTSPPT modules with capacitor reuse methodology. *IEEE TPS*, 2017, **45**(7), 1139-1145. doi:10.1109/TPS.2017.2697915.
8. Rai, K.K.; Giridhar, A.V.; Jahagirdhar, D.R.; Rai, Ashish & Paul, A.K. Mathematical modeling and analysis of high voltage high pulse power supply performance on various loads. *In* Proceedings of the 1st International Conference on Power Electronics and Energy, IEEE, India 2021. doi:10.1109/ICPEE50452.2021.9358787

9. Paul, A.K.; Giridhar, A.V.; Rai, K.K. & Kirubaharan, A. Generation of pulsed power for radar application. *In* Proceedings of the 1ˢᵗ International Conference on Power Electronics and Energy, IEEE, India, 2021. doi:10.1109/ICPEE50452.2021.9358689

10. C. -G. CHO, H. -J. RYOO, "Design of compact solid-state modulator for high–power electromagnetic pulse generation,". *In* IEEE Journal of Emerging and Selected Topics in Power Electronics, 2021, **9**(5), 6059-6068 doi:10.1109/JESTPE.2021.3079330.

CONTRIBUTORS

Mr Krishna Kumar Rai is working as Scientist in DRDO-Center For High Energy Systems and Sciences, Hyderabad. He completed his M.Tech from IIT Rourkee.
In the current study he has carried out all the literature survey, problem identification, experimental result and analysis.

Dr A.V. Giridhar received his doctorate degree from Indian Institute of Technology, Madras. He is working as Assistant Professor in the Department of Electrical Engineering, NIT, Warangal.
In the current study, he has carried out literature survey, problem identification and finding out the experimental results and validation.

Dr D.R. Jahagirdhar received his doctorate degree from Department of Electronics and Computer Science, University of Southampton, UK. He is working as Scientist in DRDO-Research Center Imarat (RCI), Hyderabad.
In the current study, he has carried out each stage of problem identification and finding out the experimental results and generation of inference.

Mr Ashish Rai completed his MTech (Microwave Electronics) from IIT (BHU). He is working as Scientist in Defence Research and Development Organization.
In the current study, he has done the hardware preparation, experimental test set up, obtaining the experimental results and result analysis.

Mr Akash Kumar Paul completed his MTech (Electrical and Electronics Engineering) from Department of Electrical Engineering, NIT, Warangal.
In the current study, he has carried out the experimental analysis and conclusion of the experiment.